Lattice vibrations in an α- and β-AgCuS superionic conductor: experimental time-of-flight inelastic neutron scattering studies

2007 J. Phys.: Condens. Matter 19 186228

(http://iopscience.iop.org/0953-8984/19/18/186228)

IOP PUBLISHING JOURNAL OF PHYSICS: CONDENSED MATTER

J. Phys.: Condens. Matter **19** (2007) 186228 (12pp) doi:10.1088/0953-8984/19/18/186228

Lattice vibrations in an α- and β-AgCuS superionic conductor: experimental time-of-flight inelastic neutron scattering studies

A N Skomorokhov[1,2,3], D M Trots[2], S G Ovchinnikov[1] and H Fuess[2]

[1] State Scientific Center—Institute for Physics and Power Engineering, Bondarenko Square 1, Obninsk 249033, Russia
[2] Insitute for Material Science, Darmstadt University of Technology, Petersenstrasse 23, Darmstadt D-64287, Germany

E-mail: romoks@mail.ru, dmytro.trots@desy.de, animate@list.ru and hfuess@tu-darmstadt.de

Received 26 September 2006, in final form 9 February 2007
Published 17 April 2007
Online at stacks.iop.org/JPhysCM/19/186228

Abstract

Inelastic neutron scattering (INS) measurements of a powder specimen of cation conducting AgCuS have been performed in its β-phase at 298 and 348 K and in its α-phase at 398 K by neutron time-of-flight (TOF) scattering. The neutron-weighted phonon density of states, $G(\varepsilon)$, of the superionic and non-superionic phases of AgCuS has been obtained. $G(\varepsilon)$ reveals a non-Debye behaviour at low energy that is caused by the presence of low-energy modes at 2.6 meV observed in the dynamic structure factor. The origin of this mode is not clear. The $\beta \rightarrow \alpha$ phase transition at 366 K is accompanied by considerable softening of several modes and simultaneous broadening of all peaks that result in a large increase of quasi-elastic intensity. Thermodynamic variables have been derived on the basis of $G(\varepsilon)$.

1. Introduction

A ternary compound of silver copper sulphide, AgCuS, has long been known to occur in nature with the mineral name stromeyerite [1–6]. The crystal structures of the low-temperature γ-phase, and the room-temperature β-phase of AgCuS with a $\gamma \rightarrow \beta$ phase transition at $\sim$250 K, were studied precisely in [7]: β- and γ-AgCuS have closely related orthorhombic symmetry with space groups $Cmc2_1$ (No. 36) and $Pmc2_1$ (No. 26). The room-temperature structure is based on the distorted hexagonal close packing of S atoms. The Cu atoms have trigonal coordination, coplanar with hexagonally packed sulfur layers. These layers are bridged by two-coordinate Ag atoms, which have large and highly anisotropic thermal motion and are bonded with near linear geometry to sulfur. The structure of γ-AgCuS differs in that the copper–sulfur sheets have become buckled and the Ag atoms are ordered into the sites either side of the

[3] Author to whom any correspondence should be addressed.

point about which they were vibrating at room temperature. The $\gamma \rightarrow \beta$ phase transition is a second-order 'order–disorder' transition with respect to the Ag sublattice, which is strongly related to changes in the lattice dynamics also. One of the major differences between the β- and γ-phases is a greatly diminished thermal motion of silver in γ-AgCuS [7]. As the temperature increases, AgCuS transforms at 366.5 K into a hexagonal α-phase, which reveals unusual physical properties, namely, anomalously high ionic conductivity. Sulfur atoms in α-AgCuS retain their hexagonal close-packed (hcp) configuration, but both silver and copper cations are disordered. However, Skarda *et al* refined the structure at $T = 388$ K by neutron powder diffraction and found that the Ag and Cu are not completely disordered [6]. Instead, most of the Cu atoms remain coplanar with sulfur as in the room-temperature phase. A next phase, appearing on further heating, is characterized by face-centred cubic (fcc) packing of sulfur [4, 5]. It is supposed that Ag and Cu ions are completely disordered in that cubic phase, though its structure has not yet ben studied [5, 6].

Originally, the main interest in AgCuS was focused on its mineralogical occurrence. Recently, the high ionic conductivity and gradual disorder in the sequential phase transitions has renewed the interest in this compound. As is known, the lattice dynamics and diffusion in superionic conductors are closely related. In particular, it is assumed that diffusion in superionics can be considered as a process connected with the low-energy optic (LEO) mode observed in the vibrational spectra of superionics [8]. Low-energy (LE) excitations have been observed by inelastic neutron scattering in the low-temperature phase of cation conducting superionics and it was suggested that the LE mode is connected with the localized vibration of the conducting type of ion [9] or with low-energy flat transverse acoustic (TA) phonons [10]. Wakamura considered the lattice dynamics in superionics based on a linear chain with two kinds of atom [10]. He showed that the value of LE excitation is related to the frequency of the transverse zone-edge acoustic phonon. This leads to the proportionality of $E_{\mathrm{LE}} \sim 1/\sqrt{m}$, where m is the heavier atomic mass. Recently, Sakuma, on the basis of INS results, has pointed out that the values of the LE excitation depend on the mass of the heaviest ion in the compound as $1/\sqrt{m}$ and not on the mass of the conducting ions [11].

It is important to consider another approach to the LE mode in superionic conductors proposed by Boyer [12]. Boyer has provided an explanation for superionicity in CaF_2, in terms of high-temperature instability of a perfect lattice [12]. It has been argued that the softening of the lowest-energy mode in CaF_2 is related to the onset of the ionic conductivity, since both effects occur at similar temperatures and lattice constants. CaF_2 has the fluorite structure, similar to many other superionic conductors where the LE mode has been observed [8–10]. At the LE mode, fluorine anions move along cubic axis directions with cage cations at rest. It is apparently of importance that neighbouring chains move out of phase. In this case fluorine ions can move in the cubic axis directions without restriction. To fit together an insufficient value of the amplitude of LE mode and the value of the minimal distance between two tetrahedral sites, Boyer has suggested that mobile ions disordered mostly over tetrahedral sites should first go in the direction of the empty octahedral sites to reduce a large potential barrier and after that jump to an adjacent tetrahedral site. The proposed mechanism of diffusion agrees with the results of [13–15] where a diffusion pathway of mobile ions in fcc superionic conductors along the tetrahedral sites in 'skewed' $\langle 100 \rangle$ directions through the peripheries of octahedral cavities was proposed.

Without doubt, the lattice dynamics and in particular the LE modes are key to understanding the phenomenon of superionicity. However, the role of the LE modes in superionic conductors is not clear. For example, recent INS measurements performed on single-crystal and powder superionic $Cu_{2-\delta}Se$ have shown no low-energy optic mode in this compound, though TA modes in $Cu_{1.85}Se$ are unusually flat over the major part of the Brillouin zone [9].

In the present work we report the results of inelastic neutron scattering studies of lattice dynamics in the powder α- and β-AgCuS superionic conductor, which to the best of our knowledge has not been studied up to now.

2. Experiments and data reduction

AgCuS powder samples were synthesized by a solid-state reaction method. The phase purity of the sample was confirmed by powder x-ray diffraction using a STOE STADI P diffractometer (Cu Kα_1 radiation, curved Ge(111) monochromator, transmission mode, step 0.03° (2θ), curved phase-sensitive detector). Calorimetric analysis was performed with simultaneous thermal analysis (STA) measurements, which combined thermogravimetry (TG) and differential scanning calorimetry (DSC). The measurements were performed using a Netzsch STA 429 device at a heating–cooling rate of 10 K min^{-1} in argon atmosphere in the 300–1000 K temperature range. The constant pressure heat capacity C_p was measured in the 3–300 K temperature range. The inelastic neutron scattering experiment was performed with the DIN-2PI time-of-flight (TOF) spectrometer of direct geometry installed at the IBR-II pulsed neutron reactor in the Joint Institute for Nuclear Research, (Dubna, Russia) [16].

The inelastic neutron scattering spectra of β-AgCuS were collected at 298, 348 K, and of α-AgCuS at 398 K. The initial neutron energy E_0 was 11.8 meV. Neutron scattering data were collected simultaneously by about 180 He^3 detectors, grouped into 12 units at constant scattering angles ϑ in the range $28° < \vartheta < 134°$. The energy resolution was about 5–8% for energy transfers between 0 and 60 meV. A polycrystalline sample (about 60 g) was placed in a hollow cylinder of 6 cm in diameter and 12 cm of height made from thin aluminium foil. The thickness of the sample was about 1–1.5 mm. The transmission of the sample was about 95%. The vacuum in the sample chamber during measurements was better than 5×10^{-2} mm Hg. Empty container and vanadium normalization measurements were also performed. The standard corrections for background due to the empty container (taking into account self-shielding), normalization and detector efficiency corrections were applied to the measured differential cross section data by the standard data reduction procedure at DIN-2PI. The neutron-weighted phonon density of states (PDOS) was obtained by an average of the generalized energy distribution function $G(Q, \varepsilon)$ over a Q range of neutron wavevector transfer of 1–7 Å^{-1}. The generalized energy distribution function $G(Q, \varepsilon)$ is related to the dynamic structure factor $S(Q, \varepsilon)$ by the relation

$$G(Q, \varepsilon) = \frac{2M}{(\hbar Q)^2} \frac{\varepsilon}{n(\varepsilon) + 1} \mathrm{e}^{2W(Q)} S(Q, \varepsilon), \tag{1}$$

where M is the mass of the scattering unit, $2W(Q)$ is the Debye–Waller exponent, and $n(\varepsilon)$ is the Bose–Einstein distribution function. The neutron-weighted PDOS, $G(\varepsilon)$, is equal to the sum of the weighted individual atom partial densities of states, $G_p(\varepsilon)$, with weighting factors $\frac{c_p \sigma_p}{M_p}$, where c_p, σ_p, M_p are the concentration, total neutron scattering cross section and mass, for the pth atomic species. For the present case, the neutron-weighted factors $\frac{c_p \sigma_p}{m_p}$ for Ag, Cu and S are 0.046, 0.125, 0.032. So contributions from thermal vibrations of all elements are observable in the experimental PDOS.

In the strict sense, the neutron-weighted PDOS includes contributions connected with multiphonon and multiple-scattering events which should be taken into account during data analysis. Multiple scattering is estimated to be very small in the total intensity of INS spectra (5% at the most) and is expected to produce a smooth background; this correction has not been taken into account. In general, the correction for multiple intensity in the case of a 95% neutron

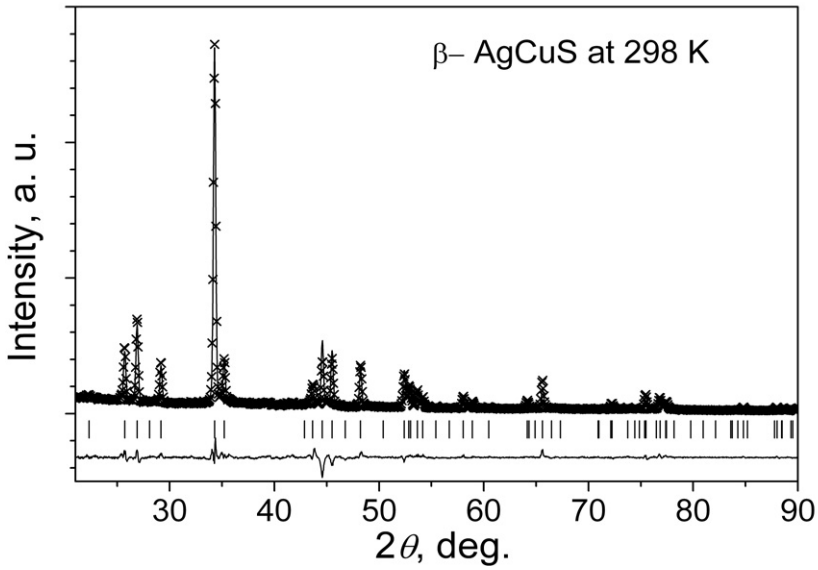

Figure 1. X-ray diffraction pattern of β-AgCuS at 298 K. The Rietveld fit is based on the model proposed in [7]. Crosses are experimental data, the line through the crosses is the calculated profile and the lower curve is their difference. Tick marks show the calculated positions of β-AgCuS Bragg reflections.

transition factor can produce only a minor effect on the result of the PDOS [17]. In contrast, the contribution connected with the multiphonon component in AgCuS could be rather high due to elevated temperatures of the measurements and a very high amplitude of thermal motion in AgCuS. A multiphonon correction procedure was applied as described in [18].

3. Data analysis and results

X-ray diffraction (XRD) analysis was performed on AgCuS at room temperature before and after the INS measurements. The XRD results reveal AgCuS as a single phase during all INS measurements and show reversibility of the α–β phase transition. At room temperature, AgCuS has the β-phase structure, in agreement with [7] (figure 1). The DSC curve of AgCuS measured in argon atmosphere displays strong endothermic signals at 370 and 936 K, which correspond to the superionic phase transition and the melting point, respectively (figure 2). The weight of the sample did not change during STA measurements within a precision of 0.2%.

The PDOSs of β-AgCuS at 298, 348 K and α-AgCuS at 398 K with calculated multiphonon and one-phonon contributions are presented in figure 3. The low-energy region ($\varepsilon < 2$ meV) where $G(\varepsilon)$ could not be analysed because of the elastic peak is shown by hatching; in this energy region $G(\varepsilon)$ was approximated by the Debye law $\sim\varepsilon^2$. The spectra of $G(\varepsilon)$ in β-AgCuS at 298 K can be described as a broad distribution up to $\sim$25 meV with two overlapped maxima at 6, 10.5 meV and a high-energy tail extended up to $\sim$42 meV. For $T = 298$ and 348 K, the resulting $G(\varepsilon)$ agree within statistical errors, which suggests a harmonic behaviour of β-AgCuS in this temperature range. For $T = 398$ K, on the other hand, there is an increase in low-energy modes below 4 meV, and at an energy above 4 meV the shape of $G(\varepsilon)$ is smeared out; peaks at $\varepsilon \sim 6$ and 10.5 meV transform to one broad distribution centred at $\sim$11 meV.

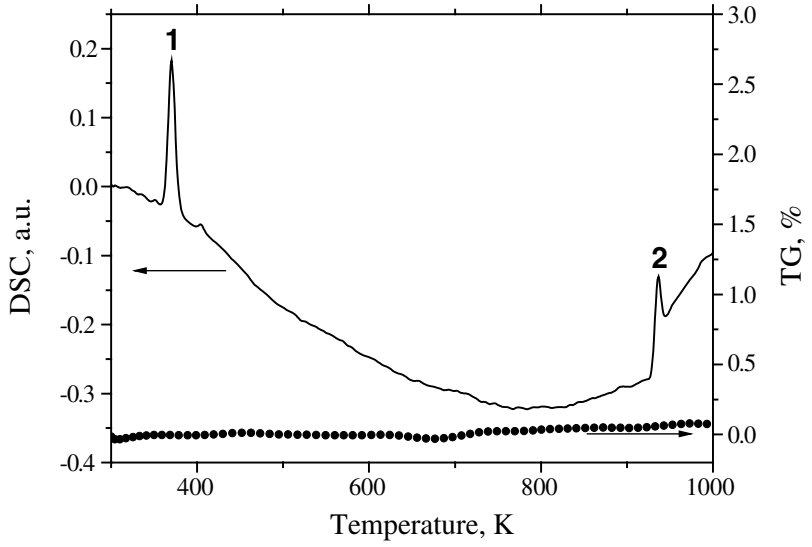

Figure 2. STA traces for AgCuS measured at a heating rate of 10 K min^{-1} in argon atmosphere. The solid line is the DSC curve, and filled circles correspond to the TG curve. Endothermic peaks (1) and (2) correspond to the $\beta \rightarrow \alpha$ superionic phase transition and melting point, respectively.

The PDOS demonstrates the linear dependence on ε at an energy $\varepsilon > 2$ meV for all three temperatures, instead of the parabolic one $G(\varepsilon) \sim \varepsilon^2$ typical of 3D solids. We can assume that the linear dependence of $G(\varepsilon) \sim \varepsilon$ is connected with the presence of the low-energy mode and resolution effects of the measurements. The lowest-energy modes were observed in INS spectra of β-AgCuS at 2.6 meV. Analysis of the angle (Q) dependence of the INS spectra was not performed because of limited statistics. To improve the statistics we present spectra of the dynamic structure factor of AgCuS at 298, 348 and 398 K in figure 4 summarized over all detectors. Peaks at 2.6 meV are seen in β-AgCuS at both sides of the spectra—the neutron energy gain and the neutron energy loss. Peaks at 6 and 10.5 meV well observable at $G(\varepsilon)$ spectra can be distinguished in the $S(\varepsilon)$ spectra as barely perceptible bending. No drastic changes in the line-shape of the $S(\varepsilon)$ spectra or shift in the peak positions take place as the temperature of the sample increases from 298 to 348 K. At the same time, as the temperature increases to $T = 398$ K the $S(\varepsilon)$ spectrum of α-AgCuS changes considerably. The low-energy part of $S(\varepsilon)$ merges with the elastic peak to become a unified broad energy distribution centred at ∼0 meV with long tails extended to 15–20 meV. The changes in $S(\varepsilon)$ at the $\beta \rightarrow \alpha$ phase transition most probably are caused by softening of low-energy modes with simultaneous increase of the peak width.

Some important lattice dynamics parameters can be obtained from the PDOS: for example, the Debye temperature Θ_{D}, lattice specific heat capacity (C_V), the mean-square displacements $\langle u^2 \rangle$ for the scattering unit and also the n-moments of the PDOS ($G^n(\varepsilon)$). The Debye temperature can be extracted from $G(\varepsilon)$ under the assumption that $G(\varepsilon)$ has Debye-like behaviour in the low-energy limit. We define the Debye model PDOS extending up to a Debye cut-off energy ε_{D} as

$$G_{\text{D}}(\varepsilon) = \begin{cases} \alpha\varepsilon^2, & \varepsilon \leqslant \varepsilon_{\text{D}} \\ 0, & \varepsilon > \varepsilon_{\text{D}} \end{cases} \tag{2}$$

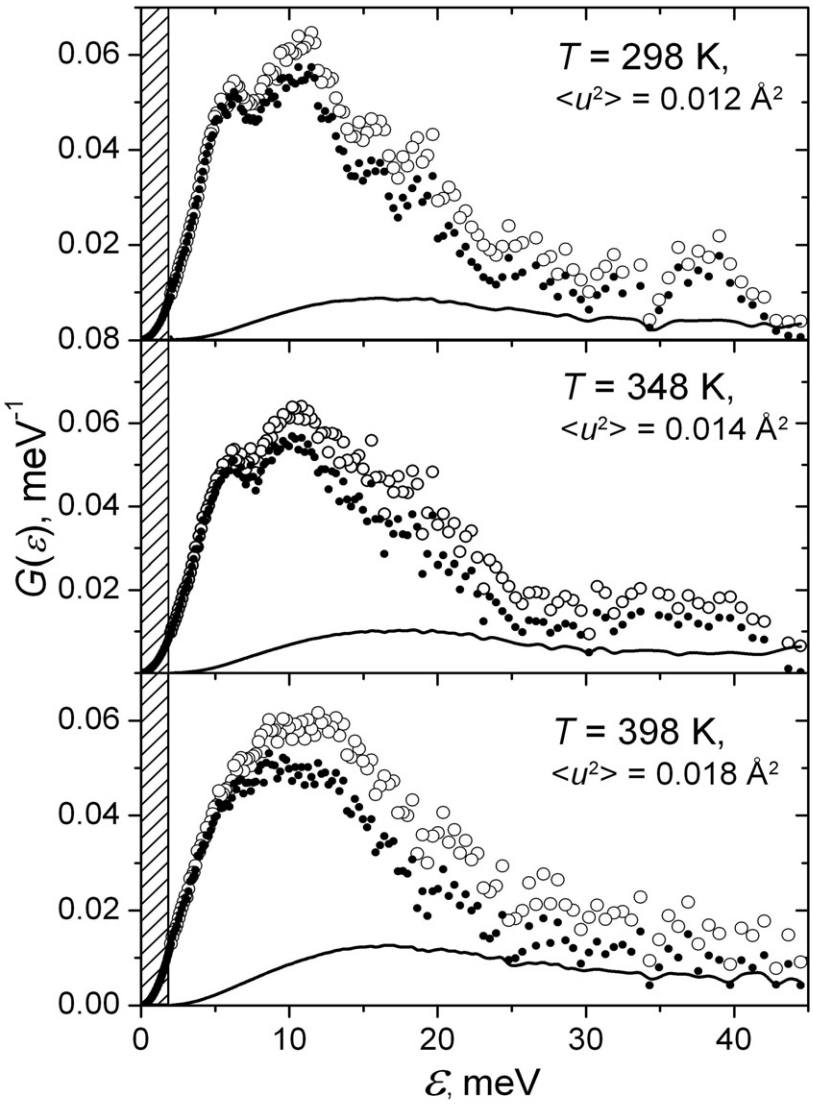

Figure 3. The PDOSs in AgCuS at 298, 348 and 398 K with one-phonon and multiphonon contributions: experiment—empty circles, one-phonon—filled circles, multiphonon contribution—solid line. The dashed region corresponds to the energy range where $G(\varepsilon)$ was interpolated to 0 according to the Debye law.

where the constant α is given by the normalization condition $\int_0^{\varepsilon_D} G(\varepsilon)\,d\varepsilon = 1$, i.e. the Debye cut-off is determined as $\frac{3}{\varepsilon_D^3} = 1$, and the Debye temperature as $\Theta_D k_B = \varepsilon_D$. $\langle u^2 \rangle$ was derived by an iteration procedure during multiphonon correction [18]. To compare results on $\langle u^2 \rangle$ obtained from $G(\varepsilon)$ with XRD results we have calculated the neutron-weighted $\langle u^2 \rangle$ from the XRD results:

$$\langle u^2 \rangle = u_{iso}^{Ag} \frac{c_{Ag}\sigma_{Ag}}{M_{Ag}} + u_{iso}^{Cu} \frac{c_{Cu}\sigma_{Cu}}{M_{Cu}} + u_{iso}^{S} \frac{c_S\sigma_S}{M_S}, \tag{3}$$

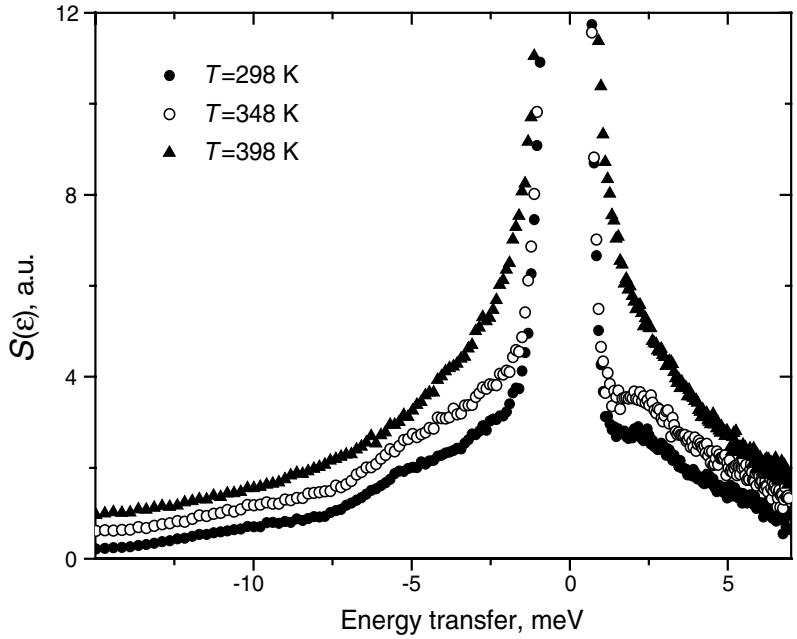

Figure 4. Dynamic structure factor of AgCuS averaged over all angles at 298, 348 and 398 K.

where u_{iso} is an isotropic thermal factor for Ag, Cu and S (see figure 7). The first and second moments of $G(\varepsilon)$ that have a clear physical meaning were determined in the usual way:

$$G^n(\varepsilon) = \int_0^{\varepsilon_{\mathrm{D}}} G(\varepsilon)\varepsilon^n \,\mathrm{d}\varepsilon. \tag{4}$$

The first momentum $G^1(\varepsilon)$ corresponds to the mean energy of the PDOS $\langle\varepsilon\rangle$ and the second one $G^2(\varepsilon)$ to mean-square energy $\langle\varepsilon^2\rangle$ that is in turn related to the mean force constant V:

$$V = \frac{M}{\hbar^2}\int_0^{\infty} G(\varepsilon)\varepsilon^2 \,\mathrm{d}\varepsilon. \tag{5}$$

If we neglect the temperature dependence of the density of states (quasi-harmonic approximation) then the constant-volume lattice specific heat per atom can be expressed as

$$C_V = 3k_{\mathrm{B}}\int_0^{\infty} G(\varepsilon)\left(\frac{\beta\varepsilon}{\mathrm{e}^{\beta\varepsilon}-1}\right)^2 \varepsilon^{\beta\varepsilon}\,\mathrm{d}\varepsilon. \tag{6}$$

The temperature dependence of the total heat capacity $C_p(T)$ derived from calorimetric measurements and the lattice heat capacity $C_v(T)$ calculated from $G(\varepsilon)$ measured at 298 K in quasi-harmonic approximation are shown in figure 5. The quite good agreement between the measured and the calculated lattice specific heat gives confirmation of the validity of the shapes and of the characteristics of the PDOS, whereas a small difference can result from anharmonic effects, electronic or other non-vibrational contributions. It should be noted that the neutron-weighted PDOS does not correspond exactly to real $G(\varepsilon)$; however, the multiphonon correction improves the agreement between $C_p(T)$ and $C_v(T)$. The lattice specific heat $C_v(T)$ calculated in the frame of the Debye model agrees with the experimental $C_p(T)$ much less than $C_v(T)$ derived from experimental neutron-weighted $G(\varepsilon)$. This demonstrates the importance of the optic mode contributions to the thermal properties of AgCuS, which are not considered in the Debye model. To analyse the heat capacity behaviour at low temperature we plot C/T versus

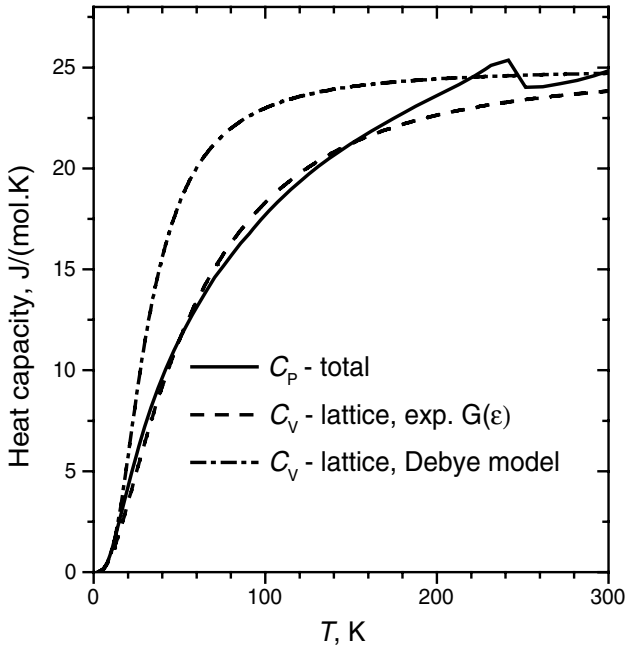

Figure 5. Experimental $C_p(T)$ obtained using the calorimetric method and lattice heat capacity $C_v(T)$ derived from $G(\varepsilon)$ in quasi-harmonic approximation. The dot–dashed line corresponds to $C_v(T)$ calculated according to the Debye model, $\Theta_D = 130$ K.

Table 1. Thermal parameters derived on the basis of $G(\varepsilon)$.

	$T = 298$ K	$T = 348$ K	$T = 398$ K
C_v (J (mol K)$^{-1}$)	23.8	24.1	24.3
Θ_D (K) $_{\varepsilon\to 0}$	125.9 ± 10	125.0 ± 10	112 ± 10
$\langle\varepsilon\rangle$ (meV)	16.4 ± 0.5	16.2 ± 0.6	16.5 ± 0.5
$\langle\varepsilon^2\rangle$ (meV^2)	381 ± 12	368 ± 15	381 ± 12
$\langle u^2\rangle$ (Å^2)	0.012 ± 0.001	0.014 ± 0.0015	0.018 ± 0.001

the temperature squared in figure 6. The low-temperature T^3 regime of the lattice specific heat does not extend beyond a few kelvins for α- and β-AgCuS, and both dependences demonstrate a negative curvature at $T > 5$ K. This is hardly surprising for the lattice specific heat because of the unusual linear dependence of $G(\varepsilon) \sim \varepsilon$ in the accessed experimental low-energy region. However, $C_p(T)/T$ demonstrates a large positive curvature at $T > 5$ K that is direct evidence of the existence of the low-energy mode in fully ordered γ-AgCuS. Linear fitting of C/T has shown the term corresponding to electronic conductivity to be equal to zero in the limit of precision.

The resulting vibrational contribution to the specific heat C_V, mean-square displacement $\langle u^2\rangle$, and the first and second moments of $G(\varepsilon)$ as representative values for 298, 348 and 398 K are given in table 1. The first and second moments of $G(\varepsilon)$, $\langle\varepsilon\rangle$ and $\langle\varepsilon^2\rangle$, at all temperatures ($T = 298$, 348 and 398 K), can be considered as coinciding results in the precision of the experiment. Values of Debye temperature and the mean-square displacement $\langle u^2\rangle$ derived

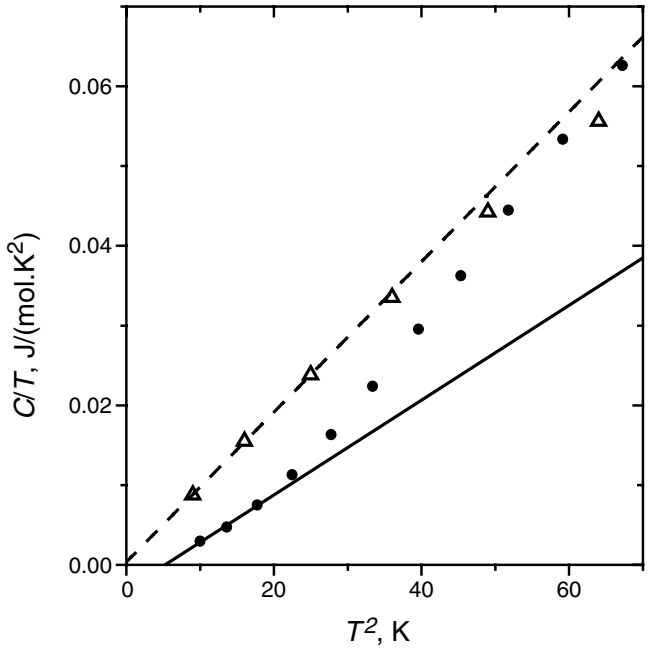

Figure 6. Total specific heat C/T of AgCuS (filled circles) and neutron-weighted lattice specific heat $C_{\rm vib}/T$ of β-AgCuS (empty triangles) derived in the quasi-harmonic approximation from $G(\varepsilon)$ at 298 K. Linear interpolation is shown by lines.

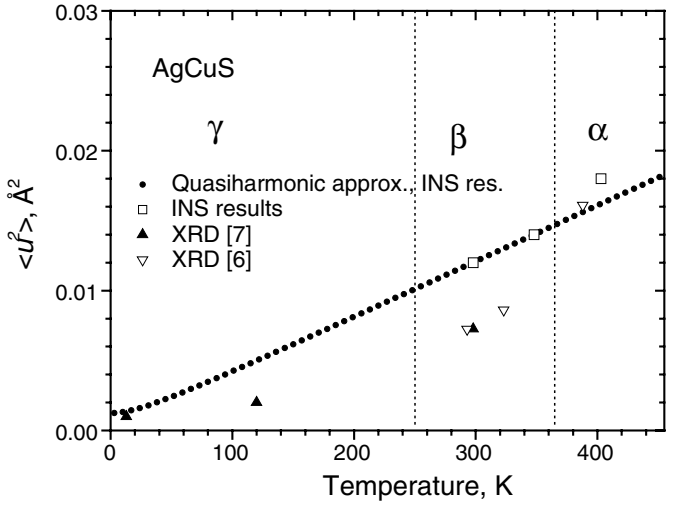

Figure 7. The neutron-weighted mean-square displacement $\langle u^2\rangle$ (AgCuS) derived from INS ($G(\varepsilon)$ at 298, 348 and 398 K) and XRD ($U_{\rm iso}$) experiments. The temperature dependence of $\langle u^2\rangle$ derived from $G(\varepsilon)$ at $T = 298$ and 348 K in the quasi-harmonic approximation is coincident (small filled circles).

at 298, 348 and 398 K are indicative of both a gradual (general) phonon softening as the temperature increases and a drastic lattice vibrational softening at the $\beta \rightarrow \alpha$ phase transition. The results of temperature dependence of $\langle u^2(T)\rangle$ derived from $G(\varepsilon)$ at 298 and 348 K in

the quasi-harmonic approximation are identical. The mean-square displacement increases with temperature within the β-phase in such a manner that linear interpolation of $\langle u^2(T)\rangle$ to low temperature results in $\langle u^2\rangle = 0$ at $T = 0$ K (see figure 7). Such a temperature dependence corresponds to harmonic behaviour of the thermal vibrations in β-AgCuS. Agreement between $G(\varepsilon)$ at 298 and 348 K shows that modifications of $S(\varepsilon)$ as the temperature increases from 298 to 348 K are related to the increase of the thermal-population factor, but are not connected with anharmonic effects. At the same time, $\langle u^2\rangle$ derived from $G(\varepsilon)$ at 398 K does not agree with a linear interpolation for $T = 298$ and 348 K, that is connected with changes in the character of thermal vibrations at the superionic phase transition. Results on $\langle u^2\rangle$ derived from XRD experiments are shown in figure 7. The agreement between the XRD and INS results is quite good. Values of $\langle u^2\rangle$ from XRD are also impossible to interpolate linearly because AgCuS at $T = 120$ and 298 K exists in different phases and also because at 13 K quantum effects in the lattice vibration are significant. Notice that $\langle u^2\rangle$ in β-AgCuS ($T = 298$, 323 K) derived from XRD data is smaller than $\langle u^2\rangle$ derived from $G(\varepsilon)$ at 298 and 348 K. According to [7], a significant feature of the structure is a large and highly anisotropic motion of Ag atoms. Since the neutron-weighted factor for silver is quite small (three times smaller than the same factor for copper), a small error in the derivation of $G(\varepsilon)$ can produce a significant error in the determination of high-amplitude vibration states. At the same time, the smaller value of $\langle u^2\rangle$ obtained on the basis of INS results may be an indication of the absence of static disorder in β-AgCuS. This is confirmation that the motion of silver would be better described by an anharmonic model rather than by static disorder [7]. The small neutron-weighted factor for silver could also be a reason why $G(\varepsilon)$ demonstrates harmonic behaviour in β-AgCuS. Actually, it is expected that the strongest anharmonic effects in AgCuS are related to thermal motion of silver atoms which is masked by its small contribution to the neutron-weighted $G(\varepsilon)$.

The Debye temperature derived in the low-energy limit from $G(\varepsilon)$ measured at 298 and 348 K coincides, and equals 125 K. The Debye temperature derived from $G(\varepsilon)$ at 398 K equals 112 K. At the same time, Θ_D derived from calorimetric measurements equals 187 K. The higher value of Θ_D obtained from calorimetric measurements is evidence that the lattice vibrations in γ-AgCuS are much harder than in β- and α-AgCuS. Hence on the basis of the INS results and heat capacity measurements we can conclude that phase transitions in AgCuS from the γ- to the β- and further to the α-phase with a gradual disordering are accompanied by considerable softening of the lattice vibrations. If we consider the invariability of the thermodynamic parameters C_V, $\langle\varepsilon\rangle$ and $\langle\varepsilon^2\rangle$ which are calculated by integration of $G(\varepsilon)$ over all the energy range of lattice vibrations, we state that the most important changes in the lattice dynamics take place at the $\beta \rightarrow \alpha$ phase transition at the low-energy part of the spectra. The most striking peculiarity of the lattice dynamics in AgCuS is the presence of a low-energy mode near 2.6 meV, which is probably connected with localized vibrations of the heaviest silver ions in AgCuS. However, strong evidence about the nature of the LE peaks can be deduced from single-crystal INS experiments. Indeed, the INS experiment performed on single-crystal $Cu_{1.85}Se$ has revealed that dispersionless LE modes observed in INS spectra of powder α- and β-$Cu_{2-\delta}Se$ are connected with the flat transverse acoustic phonons, but not with the optic mode [9]. The presence of flat acoustic phonons in AgCuS is not excluded. Such a type of acoustic phonons has been observed in binary compounds of YB_6, ZrB_{12}, LaB_6, where bonding between one type of atoms was weak [19]. On the basis of crystallographic results of AgCuS (the high value of u_{iso} for Ag, a gradual disordering of silver sublattice with temperature) we expect the bonding strength between Ag and CuS sublattice to be weak also.

4. Conclusion

In conclusion, this paper describes INS measurements of the ternary AgCuS superionic conductor in the non-superionic β- and superionic α-phases. Low-energy modes are observed in $S(\varepsilon)$ and $G(\varepsilon)$ spectra of β-AgCuS near 2.6, 6, and 10.5 meV. The neutron-weighted PDOS show a non-Debye-like behaviour for α- and β-AgCuS in the low-energy region accessed in our experiment as a result of the existence of the low-energy mode at ∼2.6 meV. The origin of this mode is not clear, but it could be related to optic-like localized vibrations of Ag ions or it could be a flat acoustic phonon. The low-temperature specific heat measurements give a strong indication of the low-energy anomaly in the PDOS of γ-AgCuS.

The dynamic structure factor changes with temperature within the β-phase ($T = 298$, 348 K) according to the thermal-population factor; the PDOS does not reveal any temperature dependence. At the $\beta \rightarrow \alpha$ phase transition the INS spectra and PDOS change considerably. The modifications of lattice dynamics at the $\beta \rightarrow \alpha$ phase transition consist of essential phonon softening and smearing of the peaks. These modifications take place, first of all, at the low-energy part of the PDOS whereas the high-energy part of the spectra does not change significantly. A consistent temperature dependence of the PDOS in β-AgCuS at 298 and 348 K and for $\langle u^2 \rangle$ indicates that the anharmonicity in the lattice dynamics of β-AgCuS is connected mostly with thermal motions of the silver ions. Single-crystal INS investigations of AgCuS as well as numerical studies of the PDOS (especially the atomic partial PDOS) are needed.

Acknowledgments

This work is supported by the Bundesministerium fuer Bildung und Forschung (German Federal Ministry of Education and Research). The authors thank C Fasel (TU Darmstadt) for performing the STA measurements and W Knafo for specific heat measurements performed in the Institute of Solid State Physics of Forschungzentrum Karlsruhe.

References

[1] Schwartz G M 1935 *Econ. Geol.* **30** 128
[2] Suhr N 1955 *Econ. Geol.* **50** 347
[3] Frueh A J 1955 *Z. Kristallogr.* **106** 299
[4] Djurle S 1958 *Acta Chem. Scand.* **12** 1427
[5] Skinner B J 1966 *Econ. Geol.* **61** 1
[6] Skarda C, Wuensch B J and Prince E 1981 *NBS Tech. Note* vol 1160, p 57
[7] Baker C L, Lincoln F J and Johnson A W S 1991 *Acta Crystallogr.* B **47** 891
[8] Sakuma T 1995 *Bull. Electrochem.* **11** 57
Hoshino S, Shapiro S M and Shibata K 1986 *J. Phys. Soc. Japan* **55** 429
Sakuma T, Shibata K and Hoshino S 1992 *Solid State Ion.* **53–56** 1278
Sakuma T and Shibata K 1989 *J. Phys. Soc. Japan* **58** 3061
Takahashi H, Hiki Y, Sakuma T and Funahashi S 1992 *Solid State Ion.* **53–56** 1164
[9] Danilkin S A, Skomorokhov A N, Hoser A, Fuess H, Rajevac V and Bickulova N N 2003 *J. Alloys Compounds* **361** 57
[10] Wakamura K 1997 *Phys. Rev.* B **56** 11593
Wakamura K 1999 *Phys. Rev.* B **59** 3560
[11] Sakuma T, Mutou M, Ohki K, Arai M, Takahashi H and Ishii Y 2002 *Solid State Ion.* **154/155** 237
[12] Boyer L L 1980 *Phys. Rev. Lett.* **45** 1858
Boyer L L 1981 *Solid State Ion.* **5** 581
[13] Keen D A 2002 *J. Phys.: Condens. Matter* **14** R819
Keen D A and Hull S 1998 *J. Phys.: Condens. Matter* **10** 8217
Keen D A and Hull S 1995 *J. Phys.: Condens. Matter* **7** 5793

Keen D A, Hull S, Barnes A C, Berastegui P, Crichton W A, Madden P A, Tucker M G and Wilson M 2003 *Phys. Rev.* B **68** 014117
[14] Skomorokhov A N, Trots D M, Knapp M, Bickulova N N and Fuess H 2006 *J. Alloys Compounds* **421** 64
[15] Trots D M, Skomorokhov A N, Knapp M and Fuess H 2006 *Eur. Phys. J.* B **51** 507
[16] Taran Yu V 1992 *User Guide. Neutron Experimental Facilities at JINR* (Dubna: JINR Press)
[17] Lindley E J and Mayers J 1988 *Neutron Scattering at a Pulsed Source* ed R J Newport, B D Rainford and R Cywinski (Bristol: Hilger)
[18] Dawidowski J, Cuello G J, Koza M M, Blostein J J, Aurelio G, Fernández Guillermet A and Donato P G 2002 *Nucl. Instrum. Methods* B **195** 389
Dawidowski J, Bermejo F J and Granada J R 1998 *Phys. Rev.* B **58** 706
[19] Mandrus D, Sales B C and Jin R 2001 *Phys. Rev.* B **64** 012302
Lortz R, Wang Y, Abe S, Meingast C, Paderno Y, Filippov V and Junod A 2005 *Phys. Rev.* B **72** 024547